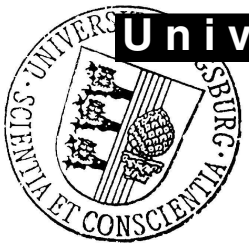

Universität Augsburg

Institut für Mathematik

Michael Hintermüller, Ronald H.W. Hoppe

Goal-Oriented Adaptivity in Pointwise State Constrained Optimal Control of Partial Differential Equations

Preprint Nr. 16/2009 — 25. Juni 2009

Institut für Mathematik, Universitätsstraße, D-86135 Augsburg http://www.math.uni-augsburg.de/

Impressum:

Herausgeber:

Institut für Mathematik
Universität Augsburg
86135 Augsburg
`http://www.math.uni-augsburg.de/pages/de/forschung/preprints.shtml`

ViSdP:

Ronald H.W. Hoppe
Institut für Mathematik
Universität Augsburg
86135 Augsburg

GOAL-ORIENTED ADAPTIVITY IN POINTWISE STATE CONSTRAINED OPTIMAL CONTROL OF PARTIAL DIFFERENTIAL EQUATIONS

MICHAEL HINTERMÜLLER * AND RONALD H.W. HOPPE †

Abstract. Primal-dual-weighted goal-oriented a posteriori error estimates for pointwise state constrained optimal control problems for second order elliptic partial differential equations are derived. The constraints give rise to a primal-dual weighted error term representing the mismatch in the complementarity system due to discretization. In the case of sufficiently regular active (or coincidence) sets and problem data, a further decomposition of the multiplier into a regular L^2-part on the active set and a singular part concentrated on the boundary between the active and inactive set allows to further characterize the mismatch error. The paper ends by a report on the behavior of the error estimates for test cases including the case of singular active sets consisting of smooth curves or points, only.

AMS subject classifications. 49K20, 65K10, 65N30, 65N50

Key words. adaptive finite element method, a posteriori error estimate, pointwise state constraints, goal-oriented adaptivity, PDE-constrained optimization

1. Introduction. This paper is devoted to mesh adaptivity for pointwise state constrained optimal control problems for elliptic partial differential equations (PDEs). A particular, unilaterally constrained model problem is given by

$$\left\{\begin{array}{ll} \text{minimize} & J(y,u) \quad \text{over } (y,u) \in H_0^1(\Omega) \times L^2(\Omega), \\ \text{subject to} & -\Delta y = u + f \quad \text{in } \Omega, \\ & y \leq b \quad \text{almost everywhere (a.e) in } \Omega, \end{array}\right. \tag{P}$$

where $\Omega \subset \mathbb{R}^n$, $n \in \{1,2,3\}$, denotes some bounded domain with sufficiently smooth boundary $\Gamma = \partial\Omega$. Further, $f \in L^2(\Omega)$ and

$$b \in W^{1,r}(\Omega), \quad \text{with} \quad b|_\Gamma > 0, \tag{1.1}$$

represent given data. A typical choice for $J : V^r \times L^2(\Omega) \to \mathbb{R}$ is given by the tracking-type objective functional

$$J(y,u) = \frac{1}{2}\|y - z\|_{0,\Omega}^2 + \frac{\alpha}{2}\|u\|_{0,\Omega}^2$$

with $\alpha > 0$ and $\|\cdot\|_{0,\Omega}$ denoting the usual norm in $L^2(\Omega)$. Further we define $V^r = H_0^1(\Omega) \cap W^{1,r}(\Omega)$ for some $r > 2$. Of course, more general objectives as well as nonlinear governing equations are conceivable.

It is well-known [6] that (P) admits a unique solution $(y^*, u^*) \in V^r \times L^2(\Omega)$ which is characterized by the following first order necessary (and in case of (P) also sufficient)

*Institute of Mathematics, Humboldt University, Unter den Linden 6, D-10099 Berlin, Germany, *hint@mathematik.hu-berlin.de*, and Department of Mathematics and Scientific Computing, University of Graz, Heinrichstraße 36, A-8010 Graz, Austria, *michael.hintermueller@uni-graz.at*. The work has been supported by the DFG Research Center MATHEON and by the Austrian Science Fund FWF under START-program Y305 "Interfaces and Free Boundaries".

†Department of Mathematics, University of Houston, Houston, TX 77204-3008, USA, *rohop@math.uh.edu*, and Institute of Mathematics, University at Augsburg, D-86159 Augsburg, Germany, *hoppe@math.uni-augsburg.de*. The work has been supported by the NSF under Grants No. DMS-0707602, DMS-0810156, and DMS-0811153.

optimality system written in weak form:

$$(\nabla y^*, \nabla v)_{0,\Omega} - (u^*, v)_{0,\Omega} = (f, v)_{0,\Omega} \quad \forall v \in H_0^1(\Omega), \tag{1.2a}$$

$$(\nabla p^*, \nabla w)_{0,\Omega} + \langle \lambda^*, w \rangle + (y, w)_{0,\Omega} = (z, w)_{0,\Omega} \quad \forall w \in V^r, \tag{1.2b}$$

$$\alpha u^* - p^* = 0, \tag{1.2c}$$

$$\langle \lambda^*, w - y^* \rangle \leq 0 \quad \forall w \in V^r \text{ with } w \leq b \text{ a.e. in } \Omega, \quad y^* \leq b \text{ a.e. in } \Omega, \tag{1.2d}$$

where $p^* \in V^s$, with $V^s = \{w \in W^{1,s}(\Omega) : w|_\Gamma = 0\}$ and $r^{-1} + s^{-1} = 1$, and $\lambda^* \in M(\bar{\Omega})$, with $M(\bar{\Omega})$ denoting the set of regular Borel measures in $\bar{\Omega}$ and $\langle \cdot, \cdot \rangle$ the duality pairing between $M(\bar{\Omega})$ and $C(\bar{\Omega})$. Note that the latter pairing is realized as

$$\langle \lambda, w \rangle = \int_{\bar{\Omega}} w \, d\lambda$$

for $\lambda \in M(\bar{\Omega})$ and $w \in V^r$. We point out that (1.2d) yields the so-called *complementarity system*

$$\lambda^* \geq 0, \quad y^* \leq b \text{ a.e. in } \Omega, \quad \langle \lambda^*, y^* - b \rangle = 0. \tag{1.3}$$

The main difficulty in the numerical treatment of (P) is related to the measure-valuedness of the Lagrange multiplier λ^*. It affects the development of efficient solution procedures as well as the derivation of error estimates and mesh adaptation techniques. Concerning the development of efficient solution algorithms we mention the recent contributions [14, 18] as well as the survey [15] and the many references therein. In [7] the convergence of a finite element discretization of (P) is established. Very recently, in [16] residual-based a posteriori error estimates for an adaptive mesh refinement in the numerical solution of (P) were derived.

Besides adaptivity guided by residual-based a posteriori error estimates in the numerical solution process, frequently one is interested in achieving accuracy with respect to a prespecified target quantity or goal. This notion leads to so-called goal-oriented adaptivity, which was pioneered in [5] for unconstrained optimal control problems. For an excellent overview over this technique we refer to [1] and to [9] for a related technique. In [11] this concept was further developed for pointwise control constrained optimal control problems. When compared to residual-based estimators, it turns out that a primal-dual weighted goal-oriented approach with the objective function as the goal allows for coarser meshes while resolving the target quantity with the same accuracy. Differently to the unconstrained case, the inequality constraints give rise to a so-called primal-dual weighted mismatch which accounts for the error when discretizing the complementarity system (related to (1.3)). This error needs to be analyzed carefully in order to avoid overestimation which would result in estimates similar to the residual-based a posteriori estimates in [13] for a class of control constrained optimal control problems.

In the present paper we study the primal-dual weighted goal-oriented approach for pointwise state constrained problems of the type (P). In contrast to the work in [11] the numerical realization of the inequalities and the discretization of the Lagrange multiplier are major issues. Based on a regularity assumption on the problem data and the active or coincidence set with respect to the inequality constraint [4], we utilize a decomposition of the multiplier into a regular L^2-part and a singular part concentrated on the boundary of the active set. This allows us to further analyze the error due to the discretization of the complementarity system (1.3). In addition, we also address the singular case where the active set consists only of a lower dimensional manifold within the domain.

The rest of the paper is organized as follows: In section 2 we derive a primal-dual-weighted error representation for our target quantity. It turns out that this representation is

not fully a posteriori. Hence, in the subsequent section 3 we establish an a posteriori error estimate up to primal-dual consistency errors. Depending on the regularity of the data and, more importantly, the coincidence or active set at the continuous solution, our analysis considers two distinct cases. In the regular case, the Lagrange multiplier pertinent to the pointwise state constraint can be decomposed into a regular L^2-part and a singular part concentrated on the boundary between the active set and its complement in Ω. In this situation we are able to further specialize the error representation. The paper ends by a report on numerical tests including the case of singular active sets.

Notation. Throughout we use $\|\cdot\|_{0,\Omega}$ and $(\cdot,\cdot)_{0,\Omega}$ for the usual $L^2(\Omega)$-norm and $L^2(\Omega)$-inner product, respectively. For convenience, with respect to the notation we shall not distinguish between the norm, respectively inner product, for scalar-valued or vector-valued arguments. We also use $(\cdot,\cdot)_{0,\mathcal{S}}$, which is the $L^2(\mathcal{S})$-inner product over a (measurable) subset $\mathcal{S} \subset \Omega$. By $|\cdot|_{1,\Omega}$ we denote the $H^1(\Omega)$-seminorm $|y|_{1,\Omega} = \|\nabla y\|_{0,\Omega}$, which, by the Poincaré-Friedrichs-inequality, is a norm on $H^1_0(\Omega)$. The norm in $H^1(\Omega)$ is written as $\|\cdot\|_{1,\Omega}$. By $\mathcal{T}_h = \mathcal{T}_h(\Omega)$ we denote a shape regular finite element triangulation of the domain Ω. The subscript $h = \max\{\mathrm{diam}(T) | T \in \mathcal{T}_h\}$ indicates the mesh size of $\mathcal{T}_h$. The vertices or nodes of the mesh are given by $\mathbf{x}_j$, $j = 1, \ldots, N_h$. The set of vertices and edges in $S \subset \Omega$ are denoted by $\mathcal{N}_h(S)$ and $\mathcal{E}_h(S)$, respectively. Finally, the notation $a \lesssim b$ implies that there exists a constant $C > 0$ (depending only on the shape regularity of the finite element triangulation) such that $a \leq C\, b$.

2. Primal-dual-weighted error representation. For deriving the structure of the new error estimate which takes into account the pointwise inequality constraints, we focus on our model problem (P). Its corresponding first order optimality characterization (1.2) can be derived from the pertinent Lagrange function $\mathcal{L} : H^1_0(\Omega) \times L^2(\Omega) \times V^s \times M(\bar\Omega) \to \mathbb{R}$ with

$$\mathcal{L}(y, u, p, \lambda) = J(y, u) + (\nabla y, \nabla p)_{0,\Omega} - (u + f, p)_{0,\Omega} + \langle \lambda, y - b \rangle. \tag{2.1}$$

For convenience we use $x := (p, y, u)$, $x^* = (p^*, y^*, u^*)$ and $X = V^s \times H^1_0(\Omega) \times L^2(\Omega)$. Obviously, the system (1.2a)–(1.2c) is equivalent to

$$\nabla_x \mathcal{L}(x^*, \lambda^*)(\varphi) = 0 \quad \forall \varphi \in X. \tag{2.2}$$

Here we consider the following finite element discretization of the problem of interest: We assume that the domain is polyhedral such that the boundary is exactly represented by boundaries of triangles T; otherwise, i.e., if Γ is a sufficiently smooth curve, the element edges lying on the boundary are assumed to be curved. By V_h we denote the space of continuous piecewise linear finite elements over $\bar\Omega$. The discrete space X_h is given by

$$X_h = V_h \times V_h \times V_h.$$

Here we use the fact that $\alpha u^* = p^*$, which implies that u^* inherits the V^s-regularity of p^*. Therefore, both quantities are discretized using the same ansatz, respectively.

For obtaining a discrete version of (1.2) we have to clarify how the discrete inequality constraint on the state is realized and, in connection with this choice, how the Lagrange multiplier is discretized. In fact, the discrete constraints read

$$y_h(a) \leq b(a) \quad \forall a \in \mathcal{N}_h(\Omega). \tag{2.3}$$

As a consequence, the discrete multiplier pertinent to (2.3) is represented by

$$\lambda_h = \sum_{a \in \mathcal{N}_h(\Omega)} \kappa_a \delta_a, \tag{2.4}$$

where δ_a denotes the Dirac measure concentrated in $a \in \mathcal{N}_h(\Omega)$. Subsequently we use

$$M_h = \{\lambda_h = \sum_{a \in \mathcal{N}_h(\Omega)} \kappa_a \delta_a \ , \ \kappa_a \in \mathbb{R} \ , \ a \in \mathcal{N}_h(\Omega)\}.$$

In order to obtain a full complementarity system (compare (1.2d)) we define I_h as the Lagrange interpolation operator associated with the nodes $a \in \mathcal{N}_h(\Omega)$, and we set

$$b_h = I_h b.$$

Now the discrete version of (1.2) is given by

$$(\nabla y_h^*, \nabla v_h)_{0,\Omega} - (u_h^*, v_h)_{0,\Omega} = (f_h, v_h)_{0,\Omega} \quad \forall v_h \in V_h, \tag{2.5a}$$
$$(\nabla p_h^*, \nabla w_h)_{0,\Omega} + \langle \lambda_h^*, w_h \rangle + (y_h, w_h)_{0,\Omega} = (z_h, w_h)_{0,\Omega} \quad \forall w_h \in V_h, \tag{2.5b}$$
$$\alpha u_h^* - p_h^* = 0, \tag{2.5c}$$
$$y_h^*(a) \le b(a), \quad \kappa_a \ge 0, \quad \forall a \in \mathcal{N}_h(\Omega), \quad \langle \lambda_h^*, y_h^* - b_h \rangle = 0. \tag{2.5d}$$

It is straightforward that (2.5) is the first order necessary and sufficient condition of the discrete version of (P) given by

$$\left\{ \begin{array}{ll} \text{minimize} & J_h(y_h, u_h) \quad \text{over } (y_h, u_h) \in V_h \times V_h, \\ \text{subject to} & (\nabla y_h, \nabla v_h)_{0,\Omega} = (u_h + f_h, v_h)_{0,\Omega} \quad \forall v_h \in V_h, \\ & y_h(a) \le b(a) \quad \forall a \in \mathcal{N}_h(\Omega), \end{array} \right. \tag{P_h}$$

where $J_h(y_h, u_h) = \frac{1}{2}\|y_h - z_h\|_{0,\Omega}^2 + \frac{\alpha}{2}\|u_h\|_{0,\Omega}^2$. The discrete Lagrangian is given by

$$\begin{aligned} \mathcal{L}_h(x_h, \lambda_h) \quad &= J_h(y_h, u_h) + (\nabla y_h, \nabla p_h)_{0,\Omega} - (u_h + f_h, p_h)_{0,\Omega} \\ &\quad + \langle \lambda_h, y_h - b_h \rangle \ . \end{aligned} \tag{2.6}$$

Similar to the continuous case, (2.5a)–(2.5c) is given by

$$\nabla_x \mathcal{L}_h(x_h^*, \lambda_h^*)(\varphi_h) = 0 \quad \forall \varphi_h \in X_h. \tag{2.7a}$$

Note that for $x \in X$, $\lambda \in \mathcal{M}(\bar{\Omega})$ and $x_h \in X_h$, $\lambda_h \in \mathcal{M}_h$ we obtain the relations

$$\mathcal{L}(x, \lambda_h) = \mathcal{L}(x, \lambda) + \langle \lambda_h - \lambda, y - b \rangle, \tag{2.8}$$
$$\nabla_x \mathcal{L}(x_h, \lambda_h)(\varphi_h) = \nabla_x \mathcal{L}(x_h, \lambda)(\varphi_h) + \langle \lambda_h - \lambda, \delta y_h \rangle \tag{2.9}$$

for all $\varphi_h = (\delta p_h, \delta y_h, \delta u_h) \in X_h$. Here we use $V^r \subset \mathcal{C}(\bar{\Omega})$ by the Sobolev embedding theorem. Moreover, for our model problem (P) the second derivative of $\mathcal{L}$ with respect to x does not depend on x and λ. Thus, we can write $\nabla_{xx}\mathcal{L}(\varphi, \hat{\varphi})$ instead of $\nabla_{xx}\mathcal{L}(x, \lambda)(\varphi, \hat{\varphi})$. Similar observations hold true for $\mathcal{L}_h$. Due to $X_h \subset X$, we have for $\varphi_h = (\delta p_h, \delta y_h, \delta u_h) \in X_h$

$$\begin{aligned} 0 &= \nabla_x \mathcal{L}(x^*, \lambda^*)(\varphi_h) \\ &= \nabla_x \mathcal{L}(x_h^*, \lambda^*)(\varphi_h) + \nabla_{xx}\mathcal{L}(x^* - x_h^*, \varphi_h) \\ &= \nabla_x \mathcal{L}(x_h^*, \lambda_h^*)(\varphi_h) + \langle \lambda^* - \lambda_h^*, \delta y_h \rangle + \nabla_{xx}\mathcal{L}(x^* - x_h^*, \varphi_h) \\ &= \nabla_x \mathcal{L}_h(x_h^*, \lambda_h^*)(\varphi_h) - (f - f_h, \delta p_h)_{0,\Omega} - (z - z_h, \delta y_h)_{0,\Omega} \\ &\quad + \langle \lambda^* - \lambda_h^*, \delta y_h \rangle + \nabla_{xx}\mathcal{L}(x^* - x_h^*, \varphi_h) \\ &= \langle \lambda^* - \lambda_h^*, \delta y_h \rangle + \nabla_{xx}\mathcal{L}(x^* - x_h^*, \varphi_h) - (f - f_h, \delta p_h)_{0,\Omega} \\ &\quad - (z - z_h, \delta y_h)_{0,\Omega}. \end{aligned} \tag{2.10}$$

From this we further derive the relations

$$\begin{aligned}\nabla_{xx}\mathcal{L}(x_h^*-x^*,x_h^*-x^*) &= \\ &= \nabla_{xx}\mathcal{L}(x_h^*-x^*,x_h^*-x^*+\varphi_h)-\langle\lambda^*-\lambda_h^*,\delta y_h\rangle \\ &\quad +(f-f_h,\delta p_h)_{0,\Omega}+(z-z_h,\delta y_h)_{0,\Omega},\end{aligned} \tag{2.11}$$

$$\nabla_x\mathcal{L}(x_h^*,\lambda^*)(x^*-x_h^*-\varphi_h)=\nabla_{xx}\mathcal{L}(x_h^*-x^*,x^*-x_h^*-\varphi_h) \tag{2.12}$$

and also

$$\begin{aligned}&\nabla_x\mathcal{L}(x_h^*,\lambda_h^*)(x^*-x_h^*-\varphi_h)= \\ &= \nabla_x\mathcal{L}(x^*,\lambda_h^*)(x^*-x_h^*-\varphi_h)+\nabla_{xx}\mathcal{L}(x_h^*-x^*,x^*-x_h^*-\varphi_h) \\ &= \langle\lambda_h^*-\lambda^*,y^*-y_h^*-\delta y_h\rangle+\nabla_{xx}\mathcal{L}(x_h^*-x^*,x^*-x_h^*-\varphi_h).\end{aligned} \tag{2.13}$$

Next we establish a representation of the difference of the continuous and discrete goal in terms of the Hessian of the Lagrangian and additional contributions.

THEOREM 2.1. *Let* $(x^*,\lambda^*)\in X\times M(\bar\Omega)$ *and* $(x_h^*,\lambda_h^*)\in X_h\times M_h$ *denote the solution of* (1.2) *and its finite dimensional counterpart* (2.5)*. Then*

$$\begin{aligned}J(y^*,u^*)-J_h(y_h^*,u_h^*) \quad &= -\tfrac12\nabla_{xx}\mathcal{L}(x_h^*-x^*,x_h^*-x^*) \\ &\quad +\langle\lambda^*,y_h^*-b\rangle+\widehat{osc}_h^{(1)},\end{aligned} \tag{2.14}$$

where the data oscillations $\widehat{osc}_h^{(1)}$ *are given by*

$$\begin{aligned}\widehat{osc}_h^{(1)} &:= \sum_{T\in\mathcal{T}_h}\widehat{osc}_T^{(1)}\,, \\ \widehat{osc}_T^{(1)} &:= (y_h^*-z_h,z_h-z)_{0,T}+\frac12\|z-z_h\|_{0,T}^2+(f_h-f,p_h^*)_{0,T}.\end{aligned} \tag{2.15}$$

Proof. Observe that $J(y^*,u^*)=\mathcal{L}(x^*,\lambda^*)$ and $J_h(y_h^*,u_h^*)=\mathcal{L}_h(x_h^*,\lambda_h^*)$. Using Taylor expansions and (2.8)-(2.9) we obtain

$$\begin{aligned}J(y^*,u^*)-J_h(y_h^*,u_h^*)&=\mathcal{L}(x^*,\lambda^*)-\mathcal{L}_h(x_h^*,\lambda_h^*)= \\ &= \mathcal{L}(x^*,\lambda^*)-\mathcal{L}_h(x^*,\lambda_h^*)-\nabla_x\mathcal{L}_h(x^*,\lambda_h^*)(x_h^*-x^*) \\ &\quad -\frac12\nabla_{xx}\mathcal{L}_h(x_h^*-x^*,x_h^*-x^*) \\ &= J(y^*,u^*)-J_h(y^*,u^*)+(f_h-f,p^*)_{0,\Omega}-\langle\lambda_h^*,y^*-b_h\rangle \\ &\quad -\nabla_x\mathcal{L}_h(x^*,\lambda_h^*)(x_h^*-x^*)-\frac12\nabla_{xx}\mathcal{L}_h(x_h^*-x^*,x_h^*-x^*) \\ &= \widehat{osc}_h^{(1)}-\langle\lambda_h^*,y^*-b_h\rangle-\nabla_x\mathcal{L}(x^*,\lambda_h^*)(x_h^*-x^*) \\ &\quad -\frac12\nabla_{xx}\mathcal{L}_h(x_h^*-x^*,x_h^*-x^*) \\ &= \widehat{osc}_h^{(1)}-\langle\lambda_h^*,y^*-y_h^*\rangle+\langle\lambda^*-\lambda_h^*,y_h^*-y^*\rangle \\ &\quad -\frac12\nabla_{xx}\mathcal{L}_h(x_h^*-x^*,x_h^*-x^*) \\ &= \widehat{osc}_h^{(1)}+\langle\lambda^*,y_h^*-b\rangle-\frac12\nabla_{xx}\mathcal{L}_h(x_h^*-x^*,x_h^*-x^*),\end{aligned}$$

where we also used the complementarity relations (1.2d) and (2.5d) as well as (2.2) and (2.7a). □

REMARK 2.1. *In the case where $\lambda^* = 0$ and $\lambda_h^* = 0$ one readily finds*

$$\begin{aligned} J(y^*,u^*) - J_h(y_h^*,u_h^*) = \frac{1}{2}\nabla_x \mathcal{L}_h(x_h^*,\lambda_h^*)(x^* - x_h^* - \varphi_h) \\ + \frac{1}{2}(f_h - f, p^* - p_h^*)_{0,\Omega} + \frac{1}{2}(z_h - z, y^* - y_h^*)_{0,\Omega} \\ + \widehat{osc}_h^{(1)} \end{aligned}$$

which corresponds to the result in [5, Proposition 4.1] for the unconstrained version of (P).

REMARK 2.2. *The contribution $\langle \lambda^*, y_h^* - b\rangle$ due to the pointwise inequality constraints can be rewritten as*

$$\langle \lambda^*, y_h^* - b\rangle = \langle \lambda^*, y_h^* - b_h\rangle + \langle \lambda^*, b_h - b\rangle. \tag{2.16}$$

Observe that (2.16) *reflects the* error in complementarity. *In fact, the second term represents the data oscillation in the upper bound on the state weighted by the continuous Lagrange multiplier, whereas the first term on the right hand side of* (2.16) *captures the* mismatch in complementarity.

We now introduce interpolation operators

$$i_h^y : V^{\bar r} \to V_h \ , \ r > \bar r > 2 \quad , \quad i_h^p : V^{\bar s} \to V_h \ , \ 1 < \bar s < s < 2, \tag{2.17}$$

such that for all $y \in V^r$ and $p \in V^s$

$$\left(h_T^{r(t-1)} \|i_h^y y - y\|_{t,r,T}^r\right)^{1/r} \lesssim \|y\|_{1,r,D_T} \ , \ 0 \le t \le 1 \ , \tag{2.18a}$$

$$\left(h_T^{-r}\|i_h^y y - y\|_{0,r,T}^r + h_T^{-r/2}\|i_h^y y - y\|_{0,r,\partial T}^r\right)^{1/r} \lesssim \|y\|_{1,r,D_T} \ , \tag{2.18b}$$

$$\left(h_T^{-s}\|i_h^p p - p\|_{0,s,T}^s + h_T^{-s/2}\|i_h^p p - p\|_{0,s,\partial T}^s\right)^{1/s} \lesssim \|p\|_{1,s,D_T} \ , \tag{2.18c}$$

where $D_T := \bigcup\{T' \in \mathcal{T}_h \mid \mathcal{N}_h(T') \cap \mathcal{N}_h(T) \neq \emptyset\}$.
Examples for interpolation operators satisfying (2.18a)-(2.18c) are the Scott-Zhang interpolation operators (cf., e.g., [19]). Now, we can further dwell on the evaluation of the Hessian of the Lagrangian and represent the error by means of *primal-dual residuals*, the *primal-dual mismatch in complementarity*, and *oscillation terms*.

THEOREM 2.2. *Let the assumptions of Theorem 2.1 be satisfied and let $i_h^z, z \in \{y, p\}$, be the interpolation operators* (2.17). *Then, the following holds:*

$$J(y^*,u^*) - J_h(y_h^*,u_h^*) = -r(i_h^z z^* - z^*) + \psi_h + \widehat{osc}_h. \tag{2.19}$$

Here, $r(i_h^z z^* - z^*)$ stands for the primal-dual-weighted residuals

$$\begin{aligned} r(i_h^z z^* - z^*) := \frac{1}{2}\Big(&(y_h^* - z_h, i_h^y y^* - y^*)_{0,\Omega} \\ &+ (\nabla(i_h^y y^* - y^*), \nabla p_h^*)_{0,\Omega} + \langle \lambda_h^*, i_h^y y^* - y^*\rangle \\ &+ (\nabla(i_h^p p^* - p^*), \nabla y_h^*)_{0,\Omega} - (u_h^* + f_h, i_h^p p^* - p^*)_{0,\Omega}\Big), \end{aligned} \tag{2.20}$$

the term ψ_h represents the primal-dual mismatch

$$\psi_h := \frac{1}{2}\big(\langle \lambda^*, y_h^* - b\rangle + \langle \lambda_h^*, b_h - y^*\rangle\big), \tag{2.21}$$

and $\widehat{osc}_h$ *refers to the data oscillations*

$$\widehat{osc}_h := \widehat{osc}_h^{(1)} + \widehat{osc}_h^{(2)}, \tag{2.22}$$

where $\widehat{osc}_h^{(1)}$ *is given by* (2.15) *and* $\widehat{osc}_h^{(2)}$ *by*

$$\widehat{osc}_h^{(2)} := \frac{1}{2}\sum_{T\in\mathcal{T}_h}\Big((f-f_h, p_h^*-p^*)_{0,T} + (z-z_h, y_h^*-y^*)_{0,T}\Big). \tag{2.23}$$

Proof. Utilizing (2.11)–(2.12) and considering $\varphi_h = (\delta p_h, \delta y_h, \delta u_h) \in X_h$ we obtain

$$\begin{aligned}
J(y^*,u^*) - J_h(y_h^*,u_h^*) &= \frac{1}{2}\nabla_{xx}\mathcal{L}(x,\lambda_h^*)(x^*-x_h^*, x_h^*-x^*+\varphi_h)\\
&\quad + \frac{1}{2}\langle\lambda^*-\lambda_h^*, \delta y_h\rangle + \frac{1}{2}(f_h-f,\delta p_h)_{0,\Omega} + \frac{1}{2}(z_h-z,\delta y_h)_{0,\Omega}\\
&\quad + \langle\lambda^*, y_h^*-b\rangle + \mathrm{osc}_h^{(1)}\\
&= -\frac{1}{2}\nabla_x\mathcal{L}(x_h^*,\lambda_h^*)(x_h^*-x^*+\varphi_h) + \frac{1}{2}\langle\lambda_h^*+\lambda^*, y_h^*-y^*\rangle\\
&\quad + \frac{1}{2}(f_h-f,\delta p_h)_{0,\Omega} + \frac{1}{2}(z_h-z,\delta y_h)_{0,\Omega} + \mathrm{osc}_h^{(1)}\\
&= -\frac{1}{2}\nabla_x\mathcal{L}_h(x_h^*,\lambda_h^*)(x_h^*-x^*+\varphi_h) + \frac{1}{2}\langle\lambda_h^*+\lambda^*, y_h^*-y^*\rangle\\
&\quad + \frac{1}{2}(f-f_h, p_h^*-p^*)_{0,\Omega} + \frac{1}{2}(z-z_h, y_h^*-y^*)_{0,\Omega} + \mathrm{osc}_h^{(1)}\,.
\end{aligned}$$

Choosing $\varphi_h = (i_h^p p^* - p_h^*, i_h^y y^* - y_h^*, i_h^u u^* - u_h^*) \in X_h$ and using complementary slackness, we continue

$$\begin{aligned}
J(y^*,u^*) - J_h(y_h^*,u_h^*) &= -\frac{1}{2}\nabla_x\mathcal{L}_h(x_h^*,\lambda_h^*)(i_h x^*-x^*) + \frac{1}{2}\big[\langle\lambda_h^*, b_h-y^*\rangle\\
&\quad + \langle\lambda^*, y_h^*-b\rangle\big] + \frac{1}{2}(f-f_h, p_h^*-p^*)_{0,\Omega} + \frac{1}{2}(z-z_h, y_h^*-y^*)_{0,\Omega}\\
&\quad + \mathrm{osc}_h^{(1)}\,.
\end{aligned}$$

The assertion now follows from (2.1) and $\alpha u_h^* - p_h^* = 0$ a.e. in Ω. ∎

We remark that so far the only easily computable term on the right-hand side in (2.19) is the oscillation term $\widehat{osc}_h^{(1)}$. All other terms still involve the unknown optimal state y^*, the optimal adjoint state p^* and/or the optimal multiplier λ^*. In the next section, we will deal with those remaining terms and provide upper bounds that are truly a posteriori in nature.

3. Primal-dual-weighted a posteriori error estimate.

3.1. Primal-dual-weighted residuals. Firstly, we are concerned with an evaluation of the primal-dual weighted residuals.

THEOREM 3.1. *Under the assumptions of Theorem 2.2 it holds that*

$$|r(i_h^z z^* - z^*)| \lesssim \sum_{T\in\mathcal{T}_h}\Big(\rho_T^{(1)}\omega_T^{(1)} + \rho_T^{(2)}\omega_T^{(2)} + \rho_T^{(3)}\omega_T^{(3)}\Big). \tag{3.1}$$

Here, for the residuals $\rho_T^{(i)}, 1\le i\le 3$, *we have*

$$\rho_T^{(1)} := \Big(\|r_T^{(1)}\|_{0,r,T}^r + h_T^{-r/2}\|r_{\partial T}^{(1)}\|_{0,r,\partial T}^r\Big)^{1/r}, \tag{3.2a}$$

$$r_T^{(1)} := u_h^* + f_h \quad , \quad r_{\partial T}^{(1)} := \frac{1}{2}\nu_{\partial T} \cdot [\nabla y_h^*] \ , \ T \in \mathcal{T}_h,$$

$$\rho_T^{(2)} := \left(\|r_T^{(2)}\|_{0,s,T}^s + h_T^{-s/2} \|r_{\partial T}^{(2)}\|_{0,r,\partial T}^s \right)^{1/s} , \tag{3.2b}$$

$$r_T^{(2)} := y_h^* - z_h \quad , \quad r_{\partial T}^{(1)} := \frac{1}{2}\nu_{\partial T} \cdot [\nabla p_h^*] \ , \ T \in \mathcal{T}_h,$$

$$\rho_T^{(3)} := \frac{1}{n_a} \sum_{a \in \mathcal{N}_h(T)} \kappa_a^* \ , \ T \in \mathcal{T}_h \ , \tag{3.2c}$$

where $n_a := card(\{T' \in \mathcal{T}_h \mid a \in \mathcal{N}_h(T')\})$ *and* $\kappa_a^*, a \in \mathcal{N}_h(\Omega)$, *are the coefficients of* λ_h^* *(cf.* (2.4)*).*
The associated weights $\omega_T^{(i)}, 1 \leq i \leq 3$, *are given by*

$$\omega_T^{(1)} := \left(\|i_h^p p^* - p^*\|_{0,s,T}^s + h_T^{s/2} \|i_h^p p^* - p^*\|_{0,s,\partial T}^s \right)^{1/s} , \tag{3.3a}$$

$$\omega_T^{(2)} := \left(\|i_h^y y^* - y^*\|_{0,r,T}^r + h_T^{r/2} \|i_h^y y^* - y^*\|_{0,r,\partial T}^r \right)^{1/r} , \tag{3.3b}$$

$$\omega_T^{(3)} := \|i_h^y y^* - y^*\|_{\frac{n}{r}+\varepsilon,r,T} \ , \ 0 < \varepsilon < \frac{r-n}{r} \ . \tag{3.3c}$$

Proof. Applying Green's formula on each element, we obtain

$$2r(i_h^z z^* - z^*) = \sum_{T \in \mathcal{T}_h} [-(r_T^{(1)}, i_h^p p^* - p^*)_{0,T} + (r_{\partial T}^{(1)}, i_h^p p^* - p^*)_{0,\partial T}] + \tag{3.4}$$
$$+ \sum_{T \in \mathcal{T}_h} [(r_T^{(2)}, i_h^y y^* - y^*)_{0,T} + (r_{\partial T}^{(2)}, i_h^y y^* - y^*)_{0,\partial T}] \ + \ \langle \lambda_h^*, i_h^y y^* - y^* \rangle \ .$$

Denoting the three terms on the right-hand side in (3.4) by I_1, I_2 and I_3, respectively, by straightforward estimation for I_1 we find

$$|I_1| \leq \sum_{T \in \mathcal{T}_h} |(r_T^{(1)}, i_h^p p^* - p^*)_{0,T}| \ + \tag{3.5}$$
$$+ |(h_T^{-1/2} r_{\partial T}^{(1)}, h_T^{1/2}(i_h^p p^* - p^*))_{0,\partial T}| \ \leq$$

$$\leq \sum_{T \in \mathcal{T}_h} [\|r_T^{(1)}\|_{0,r,T} \|i_h^p p^* - p^*\|_{0,s,T} \ + \tag{3.6}$$
$$+ h_T^{-1/2} \|r_{\partial T}^{(1)}\|_{0,r,\partial T} h_T^{1/2} \|i_h^p p^* - p^*\|_{0,s,\partial T}] \ \leq$$

$$\lesssim \sum_{T \in \mathcal{T}_h} \rho_T^{(1)} \omega_T^{(1)} \ .$$

Likewise, for I_2 we obtain

$$|I_2| \lesssim \sum_{T\in\mathcal{T}_h} \rho_T^{(2)}\omega_T^{(2)} . \tag{3.7}$$

Finally, for I_3 it follows that

$$|I_3| \le \sum_{a\in\mathcal{T}_h} \kappa_a^* \, |(i_h^y y^* - y^*)(a)| \le \sum_{T\in\mathcal{T}_h} \|i_h^y y^* - y^*\|_{C(T)} \, \frac{1}{n_a} \sum_{a\in\mathcal{N}_h(T)} \kappa_a^* .$$

Since $W^{\frac{n}{r}+\varepsilon,r}(T)$, $\varepsilon > 0$, is continuously embedded in $C(T)$, this gives

$$|I_3| \lesssim \sum_{T\in\mathcal{T}_h} \rho_T^{(3)}\omega_T^{(3)} . \tag{3.8}$$

Summing up (3.5)-(3.8) gives the assertion. □

The weights $\omega_T^{(i)}, 1 \le i \le 3$, for the residuals $\rho_T^{(i)}$ still depend on the unknown optimal state $y^* \in V^r$ and optimal adjoint state $p^* \in V^s$, respectively. One way to overcome this difficulty is to replace $i_h^y y^* - y^*$ and $i_h^p p^* - p^*$ in (3.3a)-(3.3c) by $i_H^{(2)} y_h^* - y_h^*$ and $i_H^{(2)} p_h^* - p_h^*$, where $i_H^{(2)} y_h^*$ and $i_H^{(2)} p_h^*$ are the quadratic Lagrange interpolants of y_h^*, p_h^* on a coarser mesh $\mathcal{T}_H$ with $\mathcal{T}_h \subset \mathcal{T}_H$ using the corresponding nodal values of y_h^*, p_h^* (cf., e.g., [1, 10]). Here, we proceed in a slightly different way: We replace y^*, p^* in (3.3a)-(3.3c) by y_h^*, p_h^* and denote the resulting weights by $\tilde{\omega}_T^{(i)}, 1 \le i \le 3$, i.e., we define

$$\tilde{\omega}_T^{(1)} := \left(\|i_h^p p_h^* - p_h^*\|_{0,s,T}^s + h_T^{s/2} \|i_h^p p_h^* - p_h^*\|_{0,s,\partial T}^s \right)^{1/s} , \tag{3.9a}$$

$$\tilde{\omega}_T^{(2)} := \left(\|i_h^y y_h^* - y_h^*\|_{0,r,T}^r + h_T^{r/2} \|i_h^y y_h^* - y_h^*\|_{0,r,\partial T}^r \right)^{1/r} , \tag{3.9b}$$

$$\tilde{\omega}_T^{(3)} := \|i_h^y y_h^* - y_h^*\|_{\frac{n}{r}+\varepsilon,r,T} , \; 0 < \varepsilon < \frac{r-n}{r} . \tag{3.9c}$$

Further, using the approximation properties (2.18a)-(2.18c), we obtain the computable upper bounds

$$\tilde{\omega}_T^{(1)} \lesssim \hat{\omega}_T^{(1)} := h_T \, \|p_h^*\|_{1,s,D_T} , \tag{3.10a}$$

$$\tilde{\omega}_T^{(2)} \lesssim \hat{\omega}_T^{(2)} := h_T \, \|y_h^*\|_{1,r,D_T} , \tag{3.10b}$$

$$\tilde{\omega}_T^{(3)} \lesssim \hat{\omega}_T^{(3)} := h_T^{(1-\varepsilon)-n/r} \|y_h^*\|_{1,r,D_T} , \; 0 < \varepsilon < \frac{r-n}{r} . \tag{3.10c}$$

Substituting $\omega_T^{(i)}$ by $\hat{\omega}_T^{(i)}, 1 \le i \le 3$, we obtain the *primal-dual weighted a posteriori error estimator*

$$\eta_h^{PD} := \sum_{T\in\mathcal{T}_h} \eta_T^{PD} , \tag{3.11}$$

$$\eta_T^{PD} := \sum_{i=1}^{3} \rho_T^{(i)} \hat{\omega}_T^{(i)} , \; T \in \mathcal{T}_h .$$

3.2. Primal-dual mismatch in complementarity. The term $\psi(y^*, y_h^*)$ as given by (2.21) is again related to errors coming from complementary slackness. For its interpretation, we define the active set $\mathcal{A}^*$ and the inactive set $\mathcal{I}^*$ at the optimal solution (x^*, λ^*) of (P) by

$$\mathcal{A}^* := \{\mathbf{x} \in \Omega : y^*(\mathbf{x}) = b(\mathbf{x})\}, \quad \mathcal{I}^* := \Omega \setminus \mathcal{A}^*. \tag{3.12}$$

The discrete analogues of $\mathcal{A}^*$ and $\mathcal{I}^*$ are defined as follows: First, let

$$A_h^* := \{j \in \{1, \dots, N_h\} : y_h^*(\mathbf{x}_j) = b(\mathbf{x}_j)\}, \quad I_h^* := \{1, \dots, N_h\} \setminus \mathcal{A}_h^*. \tag{3.13}$$

denote the active and inactive vertices, respectively. Then the discrete active and inactive sets are respectively defined by

$$\mathcal{A}_h^* := \{T \in \mathcal{T}_h(\Omega) : \mathcal{N}_h(T) \subset A_h^*\}, \quad \mathcal{I}_h^* := \mathcal{T}_h(\Omega) \setminus \mathcal{A}_h^*. \tag{3.14}$$

Next we define $J^* = \{j \in \{1, \dots, N_h\} : \mathbf{x}_j \in \mathcal{I}^*\}$. Then we have

$$\langle \lambda_h^*, b_h - y^* \rangle = \langle \lambda_h^*, b - y^* \rangle = \sum_{j \in J^*} \kappa_j^* \left(b(\mathbf{x}_j) - y^*(\mathbf{x}_j)\right) \geq 0$$

since $b_h(\mathbf{x}_j) = b(\mathbf{x}_j)$ for all $j = 1, \dots, N_h$. Here and below, we use κ_j^* instead of $\kappa_{\mathbf{x}_j}^*$ for $\mathbf{x}_j \in \mathcal{N}_h(\Omega)$. Hence, the right hand side above represents the *primal-dual weighted mismatch in complementarity in* $\mathcal{I}^*$.
Due to the continuous and discrete complementarity systems (1.2d) and (2.5d), ψ_h is equivalent to

$$\psi_h = \frac{1}{2}\big[\langle \lambda_h^* - \lambda^*, b_h - y^* \rangle + \langle \lambda_h^* - \lambda^*, b - y_h^* \rangle + \langle \lambda_h^* + \lambda^*, b_h - b \rangle\big]. \tag{3.15}$$

Recall that $\langle \lambda_h^*, y_h^* - b \rangle = \langle \lambda_h^*, y_h^* - b_h \rangle = 0$ as well as $\langle \lambda_h^*, b - b_h \rangle = 0$ for any $\lambda_h \in \mathcal{M}_h$. These facts would allow us to simplify the above expression even further. For our subsequent treatment of the dual products on the right-hand side in (3.15), following [4] we will consider the so-called regular and non-regular cases with regard to a classification of the structure of the Lagrange multiplier associated with the state-constrained optimal control problem.

3.2.1. Regular case. We assume that the coincidence set $\mathcal{A}^*$ satisfies

$$\left\{ \begin{array}{l} \mathcal{A}^* = \bigcup_{i=1}^m \mathcal{A}_i^*, \quad \text{cl}(\text{int}(\mathcal{A}_i^*)) = \mathcal{A}_i^*, \quad 1 \leq i \leq m, \\ \mathcal{A}_i^* \cap \mathcal{A}_j^* = \emptyset, \quad 1 \leq i \neq j \leq m, \\ \mathcal{A}_i^*,\ 1 \leq i \leq m, \text{ is connected with } C^{1,1}\text{-boundary}. \end{array} \right. \tag{A_1}$$

Since $\mathcal{A}^* \cap \Gamma = \emptyset$ is already implied by our assumption (1.1) on the data, i.e., a Slater condition for (P), in view of [4, Thm.2] we have

$$p^* \in V, \quad p^*|_{int(\mathcal{A}^*)} \in H^2(\text{int}(\mathcal{A}^*)), \quad p^*|_{\mathcal{I}^*} \in H^2(\mathcal{I}^*) \tag{3.16}$$

and

$$p^* = -\alpha\, \Delta b \quad \text{in } \mathcal{A}^*, \tag{3.17a}$$

$$-\Delta p^* = z - y^* \quad \text{in } \mathcal{I}^*, \tag{3.17b}$$

$$p^* = -\alpha\, \Delta b \quad \text{on } \mathcal{F}^*,$$

$$\lambda^* = \mu^* + \mu_{\mathcal{F}^*}^*, \quad \mu^* \in L_+^2(\Omega)\ ,\ \mu_{\mathcal{F}^*}^* \in H_+^{1/2}(\mathcal{F}^*), \tag{3.17c}$$

where

$$\mu^* = \begin{cases} 0 & \text{on } \mathcal{I}^*, \\ z - b - \alpha\,\Delta^2 b & \text{on } \mathcal{A}^*, \end{cases} \tag{3.18a}$$

$$\mu^*_{\mathcal{F}^*} = -\frac{\partial p^*|_{\mathcal{I}^*}}{\partial n_{\mathcal{I}^*}} + \alpha \frac{\partial \Delta b}{\partial n_{\mathcal{A}^*}}, \tag{3.18b}$$

and $L^2_+(\Omega)$ as well as $H^{1/2}_+(\mathcal{F}^*)$ denote the non-negative cones in $L^2(\Omega)$ and $H^{1/2}(\mathcal{F}^*)$, respectively.
Following [12] (see also [13, 17]), we estimate the continuous coincidence set $\mathcal{A}^*$ by

$$\chi_h^{\mathcal{A}^*} \;:=\; I - \frac{b - i_h^y y_h^*}{\gamma h^r + b - i_h^y y_h^*}\,,$$

where $0 < \gamma \leq 1$ and $r > 0$ are fixed. Denoting by $\chi(S)$ the characteristic function of $S \subset \Omega$, for $T \subset \mathcal{A}^*$ we find

$$\|\chi(\mathcal{A}^*) - \chi_h^{\mathcal{A}^*}\|_{0,T} \;\leq\; \min(|T|^{1/2}, \gamma^{-1} h^{-r} \|y^* - i_h^y y_h^*\|_{0,T})$$

which converges to zero whenever $\|y^* - i_h^y y_h^*\|_{0,T} = O(h^q), q > r$. Likewise, for $T \subset \mathcal{I}^*$ one can show as well that $\|\chi(\mathcal{A}^*) - \chi_h^{\mathcal{A}^*}\|_{0,T} \to 0$ as $h \to 0$. Now, for fixed $0 < \kappa \leq 1$ and $0 < s \leq r$ we provide approximations $\hat{\mathcal{A}}_h^*$ of $\mathcal{A}^*$ and $\hat{\mathcal{I}}_h^*$ of $\mathcal{I}^*$ according to

$$\hat{\mathcal{A}}_h^* := \bigcup \{T \in \mathcal{T}_h \mid \chi_h^{\mathcal{A}^*}(x) \geq 1 - \kappa h^s \text{ for all } x \in T\}\,, \tag{3.19a}$$

$$\hat{\mathcal{I}}_h^* := \bigcup \{T \in \mathcal{T}_h \mid \chi_h^{\mathcal{A}^*}(x) < 1 - \kappa h^s \text{ for some } x \in T\}\,. \tag{3.19b}$$

We define approximations $\mathcal{T}_{\mathcal{A}^* \cap \mathcal{A}_h^*}, \mathcal{T}_{\mathcal{I} \cap \mathcal{A}_h^*}$ and $\mathcal{T}_{\mathcal{A}^* \cap \mathcal{I}_h^*}$ of $\mathcal{A}^* \cap \mathcal{A}_h^*, \mathcal{I}^* \cap \mathcal{A}_h^*$ and $\mathcal{A}^* \cap \mathcal{I}_h^*$ by means of

$$\mathcal{T}_{\mathcal{A}^* \cap \mathcal{A}_h^*} := \hat{\mathcal{A}}_h^* \cap \mathcal{A}_h^*, \quad \mathcal{T}_{\mathcal{I}^* \cap \mathcal{A}_h^*} := \hat{\mathcal{I}}_h^* \cap \mathcal{A}_h^*, \quad \mathcal{T}_{\mathcal{A}^* \cap \mathcal{I}_h^*} := \hat{\mathcal{A}}_h^* \cap \mathcal{I}_h^*\,,$$

If int $\hat{\mathcal{I}}_h^* \neq \emptyset$ and int $\hat{\mathcal{A}}_h^* \neq \emptyset$, we introduce

$$\mu_{\hat{\mathcal{F}}_h^*} := -\frac{\partial p_h^*|_{\hat{\mathcal{I}}_h^*}}{\partial n_{\hat{\mathcal{I}}_h^*}} + \alpha\,\frac{\partial \Delta b}{\partial n_{\hat{\mathcal{A}}_h^*}} \tag{3.20}$$

as an approximation of (3.18b), where $\hat{\mathcal{F}}_h^* := \partial \hat{\mathcal{A}}_h^* \cap \hat{\mathcal{I}}_h^*$. Based on (3.17a)-(3.17c), (3.18a), (3.18b) and (3.20) we are able to evaluate ψ_h for the four sets $\mathcal{I}^* \cap \mathcal{I}_h^*, \mathcal{A}^* \cap \mathcal{A}_h^*, \mathcal{A}^* \cap \mathcal{I}_h^*, \mathcal{I}^* \cap \mathcal{A}_h^*$.
Case 1 ($\mathcal{I}^* \cap \mathcal{I}_h^*$): Due to $\mu^* = 0$ on $\mathcal{I}^*$ and $\lambda_h^* = 0$ on $\mathcal{I}_h^*$, we obviously have

$$\psi_h|_{\mathcal{I}^* \cap \mathcal{I}_h^*} = \frac{1}{2}\Big(\sum_{a \in \mathcal{N}_h(\mathcal{F}_h^* \cap \mathcal{I}^*)} \kappa_a^*(y_h^* - y^*)(a) + (\mu^*|_{\mathcal{F}^*}, y_h^* - b)_{0, \mathcal{F}^* \cap \mathcal{I}_h^*} \Big). \tag{3.21}$$

Since y^* is unknown, following [1] we approximate $y^*|_T$ by $\hat{y}_\ell^*|T, T \in \mathcal{T}_h(\Omega)$, where this approximation is obtained in the following way: Assuming that the triangulation $\mathcal{T}_h(\Omega)$ stems from the refinement of a coarser triangulation $\mathcal{T}_H(\Omega)$, we consider the 'father' $T_F \in \mathcal{T}_H(\Omega)$ of $T \in \mathcal{T}_h(\Omega)$ and define $\hat{y}_\ell^*$ as the quadratic interpolant of y_ℓ^* on T_F with respect to the

nodal values in the vertices and the midpoints of the edges of T_F. This leads to the following approximations:

$$\hat{\psi}_h^{(1)} := \sum_{T\in\mathcal{T}_h} \hat{\psi}_T^{(1)} \,, \tag{3.22}$$

$$\hat{\psi}_T^{(1)} := \begin{cases} \frac{1}{4}\|\mu_{\hat{\mathcal{F}}_h^*}\|_E \|y_h^* - b\|_E \,, T \in \{T_\pm\}, E = T_+ \cap T_- \in \mathcal{E}_h(\hat{\mathcal{F}}_h^*), \\ 0, \,, \qquad \text{otherwise,} \end{cases}$$

$$\hat{\psi}_h^{(2)} := \sum_{T\in\mathcal{T}_h} \hat{\psi}_T^{(2)} \,, \tag{3.23}$$

$$\hat{\psi}_T^{(2)} := \begin{cases} \frac{1}{2} \sum\limits_{a\in\mathcal{N}_h(T)} |y_h^* - \hat{y}_h^*)(a)|\kappa_a^* \,, T \in \mathcal{T}_{\hat{\mathcal{F}}_h^*\cap\hat{\mathcal{I}}_h^*}, \\ 0 \,, \quad \text{otherwise,} \end{cases}$$

and thus arrive at the upper bound

$$\hat{\psi}_h|_{\hat{\mathcal{I}}_h^*\cap\mathcal{I}_h^*} = \hat{\psi}_h^{(1)} + \hat{\psi}_h^{(2)}. \tag{3.24}$$

Case 2 ($\mathcal{A}^* \cap \mathcal{A}_h^*$): In view of $y^* = b, y_h^* = b_h$ on $\mathcal{A}^* \cap \mathcal{A}_h^*$ and (3.17c), we obtain

$$\psi_h|_{\mathcal{A}^*\cap\mathcal{A}_h^*} = \frac{1}{2}\Big((z - b - \alpha\Delta^2 b, b_h - b)_{0,\mathcal{A}^*\cap\mathcal{A}_h^*} + (\mu_{\mathcal{F}^*}^*, b_h - b)_{0,\mathcal{F}^*\cap\mathcal{A}_h^*}\Big). \tag{3.25}$$

We introduce the approximation

$$\hat{\psi}^{(3)} := \sum_{T\in\mathcal{T}_h} \hat{\psi}_T^{(3)} \,, \tag{3.26}$$

$$\hat{\psi}_T^{(3)} := \begin{cases} \frac{1}{2}\|z - b - \alpha\Delta^2 b\|_T \|b - b_h\|_T \,, T \in \mathcal{T}_{\hat{\mathcal{A}}_h^*\cap\mathcal{A}_h^*}, \\ 0 \,, \quad \text{otherwise,} \end{cases}$$

and thus get the upper bound

$$\hat{\psi}_h|_{\hat{\mathcal{A}}_h^*\cap\mathcal{A}_h^*} = \hat{\psi}_h^{(1)} + \hat{\psi}_h^{(3)}. \tag{3.27}$$

Case 3 ($\mathcal{A}^* \cap \mathcal{I}_h^*$): Taking $y^* = b$ on $\mathcal{A}^*$, and $\lambda_h^* = 0$ on $\mathcal{I}_h^*$ and (3.17a),(3.17b) into account, we get

$$\psi_h|_{\mathcal{A}^*\cap\mathcal{I}_h^*} = \frac{1}{2}\Big((\mu^*, y_h^* - b)_{0,\mathcal{A}^*\cap\mathcal{I}_h^*} + (\mu_{\mathcal{F}^*}^*, y_h^* - b)_{0,\mathcal{F}^*\cap\mathcal{I}_h^*}\Big). \tag{3.28}$$

Setting

$$\hat{\psi}_h^{(4)} := \sum_{T\in\mathcal{T}_h} \hat{\psi}_T^{(4)} \,, \tag{3.29}$$

$$\hat{\psi}_T^{(4)} := \begin{cases} \frac{1}{2}\|z - b - \alpha\Delta^2 b\|_T \|y_h^* - b\|_T \,, T \in \mathcal{T}_{\hat{\mathcal{A}}_h^*\cap\mathcal{I}_h^*}, \\ 0 \,, \quad \text{otherwise,} \end{cases}$$

it follows that an upper bound is given by

$$\hat{\psi}_h|_{\hat{\mathcal{A}}_h^*\cap\mathcal{I}_h^*} = \hat{\psi}_h^{(1)} + \hat{\psi}_h^{(4)}. \tag{3.30}$$

Case 4 ($\mathcal{I}^* \cap \mathcal{A}_h^*$): Finally, observing $\mu^* = 0$ on $\mathcal{I}^*$ and $y_h^* = b_h$ on $\mathcal{A}_h^*$ as well as (3.17a),(3.17b), for the fourth set we have

$$\psi_h|_{\mathcal{I}^*\cap\mathcal{A}_h^*} == \frac{1}{2}\Big(\sum_{a\in\mathcal{N}_h(\mathcal{I}^*\cap\mathcal{A}_h^*)} \kappa_a^*(y_h^* - y^*)(a) + (\mu_{\mathcal{F}^*}^*, b_h - b)_{0,\mathcal{F}^*\cap\mathcal{A}_h^*}\Big). \tag{3.31}$$

Introducing the approximation

$$\hat{\psi}_h^{(5)} := \sum_{T\in\mathcal{T}_h} \hat{\psi}_T^{(5)}\,, \tag{3.32}$$
$$\hat{\psi}_T^{(5)} := \begin{cases} \frac{1}{2} \sum\limits_{a\in\mathcal{N}_h(T)} |y_h^* - \hat{y}_h^*)(a)|\kappa_a^*\,, T \in \mathcal{T}_{\mathcal{I}_h^*\cap\mathcal{A}_h^*}, \\ 0\,, \quad \text{otherwise}, \end{cases}$$

we obtain the upper bound

$$\hat{\psi}_h|_{\hat{\mathcal{I}}_h^*\cap\mathcal{A}_h^*} = \hat{\psi}_h^{(1)} + \hat{\psi}_h^{(5)}. \tag{3.33}$$

3.2.2. Nonregular case. The non-regular case assumes the following structure of the active set $\mathcal{A}^*$:

$$\mathcal{A}^* \text{ is a Lipschitzian, strongly non-self-intersecting curve in } \Omega \quad . \tag{A_2}$$

We note that a curve $\mathcal{C}$ is said to be strongly non-self-intersecting, if, for every $a \in \text{int}(\mathcal{C})$, there exists an open neighborhood $\mathcal{U}(a)$ such that $\mathcal{U}(a) \setminus \mathcal{C}$ consists of two connected components. Hence, $\mathcal{A}^*$ divides Ω into two connected components Ω_+ and Ω_-.
Again, since the Slater condition (1.1) implies $\mathcal{A}^* \cap \Gamma = \emptyset$, [4, Thm.4] provides the following optimality characterization:

$$(\nabla p^*, \nabla w)_{0,\Omega} = (z - y^*, w) - \langle \lambda^*, w\rangle\,,\ w \in W^{1,r}(\Omega), \tag{3.34a}$$
$$\lambda^* = \mu_{\mathcal{A}^*}^* = \nu_{\mathcal{A}^*} \cdot \nabla p^*|_{\mathcal{A}_+^*} - \nu_{\mathcal{A}^*} \cdot \nabla p^*|_{\mathcal{A}_-^*}\,, \tag{3.34b}$$

where $\nu_{\mathcal{A}^*}$ denotes the unit outer normal to $\mathcal{A}^*$ pointing towards $\mathcal{A}_+^* := \mathcal{A}^* \cap \bar{\Omega}_+$ and $\mathcal{A}_-^* := \mathcal{A}^* \cap \bar{\Omega}_-$.

We further define $\mu_{\hat{\mathcal{F}}_h^*}^*$ according to

$$\mu_{\hat{\mathcal{F}}_h^*}^* := \begin{cases} \nu_{\mathcal{A}_h^*} \cdot \nabla p_h^*|_{\mathcal{A}_h^*} - \nu_{\mathcal{I}_h^*} \cdot \nabla p_h^*|_{\mathcal{I}_h^*}\,, \text{if meas}(\mathcal{A}_h^*) > 0, \\ \nu_{\mathcal{A}_h^*} \cdot \nabla p_h^*|_{\mathcal{A}_{h,+}^*} - \nu_{\mathcal{A}_h^*} \cdot \nabla p_h^*|_{\mathcal{A}_{h,-}^*}\,, \text{if meas}(\mathcal{A}_h^*) = 0, \end{cases} \tag{3.35}$$

where, for $\text{meas}(\mathcal{A}_h^*) = 0$, $\nu_{\mathcal{A}_h^*}$ and $\mathcal{A}_{h,\pm}^*$ are defined as in the continuous case.

As in the regular case, we evaluate ψ_h for the four sets $\mathcal{I}^*\cap\mathcal{I}_h^*, \mathcal{A}^*\cap\mathcal{A}_h^*, \mathcal{A}^*\cap\mathcal{I}_h^*, \mathcal{I}^*\cap\mathcal{A}_h^*$. We refer to $\hat{\psi}_h^{(1)}, \hat{\psi}_h^{(2)}$ and $\hat{\psi}_h^{(5)}$ as the error bounds given by (3.22), (3.23) and (3.32) with $\mu_{\hat{\mathcal{F}}_h^*}^*$ in (3.22) replaced by (3.35).

Case 1 ($\mathcal{I}^* \cap \mathcal{I}_h^*$): We have

$$\hat{\psi}_h|_{\mathcal{I}_h^*\cap\mathcal{I}_h^*} = \hat{\psi}_h^{(1)} + \hat{\psi}_h^{(2)}. \tag{3.36}$$

Case 2 ($\mathcal{A}^* \cap \mathcal{A}_h^*$): We infer the upper bound

$$\hat{\psi}_h|_{\hat{\mathcal{A}}_h^*\cap\mathcal{A}_h^*} = \hat{\psi}_h^{(1)}. \tag{3.37}$$

Case 3 ($\mathcal{A}^* \cap \mathcal{I}_h^*$): As in the second case we obtain

$$\hat{\psi}_h|_{\hat{\mathcal{A}}_h^* \cap \mathcal{I}_h^*} = \hat{\psi}_h^{(1)}. \tag{3.38}$$

Case 4 ($\mathcal{I}^* \cap \mathcal{A}_h^*$): We get the upper bound

$$\hat{\psi}_h|_{\hat{\mathcal{I}}_h^* \cap \mathcal{A}_h^*} = \hat{\psi}_h^{(1)} + \hat{\psi}_h^{(5)}. \tag{3.39}$$

3.3. Primal-dual weighted data oscillations. The data oscillation term $\widehat{osc}_h^{(2)}$ as given by (2.23) can be estimated by means of

$$\begin{aligned} \widehat{osc}_h^{(2)} &= \sum_{T \in \mathcal{T}_h} \widehat{osc}_T^{(2)}, \\ \widehat{osc}_T^{(2)} &:= \|f - f_h\|_{0,T} \|p_h^* - \hat{p}_h^*\|_{0,T} + \|z - z_h\|_{0,T} \|y_h^* - \hat{y}_h^*\|_{0,T}, \end{aligned} \tag{3.40}$$

where $\hat{p}_h^*$ is defined in the same way as $\hat{y}_h^*$ before (cf. Section 3.2.1, Case 1).
We thus obtain the following upper bound for the data oscillations

$$\widehat{osc}_h := \widehat{osc}_h^{(1)} + \widehat{osc}_h^{(2)}. \tag{3.41}$$

4. The adaptive algorithm. The adaptive finite element algorithm based on the goal-oriented dual weighted residuals consists of successive loops of the cycle

$$\text{SOLVE} \quad \Longrightarrow \quad \text{ESTIMATE} \quad \Longrightarrow \quad \text{MARK} \quad \Longrightarrow \quad \text{REFINE}\,.$$

Here, SOLVE stands for the numerical solution of the discrete optimality system (2.5a)-(2.5d) which is taken care of by the primal-dual active set strategy from [3]. The following step ESTIMATE requires the computation of the upper bounds for the weighted dual residuals, the primal-dual mismatch in complementarity, and the data oscillations as derived in the previous section 3. The following step MARK takes care of the selection of elements of the triangulation $\mathcal{T}_h$ for refinement based on the information provided by the weighted dual residuals and the upper bounds for the primal-dual mismatch in complementarity and the data oscillations. For this selection process, we use a bulk criterion, also known as Dörfler marking [8] which will be described here in the regular case (the modifications in the nonregular case are obvious). Referring to $\rho_T^{(i)}, \hat{\omega}_T^{(i)}, 1 \le i \le 3$, $\hat{\psi}_T^{(i)}, 1 \le i \le 5$, and $\widehat{osc}_T^{(i)}, 1 \le i \le 2$, as the residuals (3.2a)-(3.2c) and upper bounds as given by (3.3a)-(3.3c), (3.22),(3.23),(3.26),(3.29),(3.32), and (2.15),(3.40), we select a subset $\hat{\mathcal{T}}_h$ of elements such that for some universal constant $0 < \Theta < 1$ there holds

$$\begin{aligned} &\Theta \sum_{T \in \mathcal{T}_h} \Big(\sum_{i=1}^{3} \rho_T^{(i)} \hat{\omega}_T^{(i)} + \sum_{i=1}^{5} \hat{\psi}_T^{(i)} + \sum_{i=1}^{2} \widehat{osc}_T^{(i)} \Big) \\ &\le \sum_{T \in \hat{\mathcal{T}}_h} \Big(\sum_{i=1}^{3} \rho_T^{(i)} \hat{\omega}_T^{(i)} + \sum_{i=1}^{5} \hat{\psi}_T^{(i)} + \sum_{i=1}^{2} \widehat{osc}_T^{(i)} \Big)\,. \end{aligned} \tag{4.1}$$

The bulk criterion can be realized by a greedy algorithm [13]. The final step REFINE is devoted to the technical realization of the refinement process.

5. Numerical results. We present the numerical results for two test examples to illustrate the performance of the adaptive algorithm described in section 4. The first example represents a problem where the coincidence set consists of a simply-connected subdomain with a smooth boundary and the origin. It fits the setting of the regular case treated in section 3, whereas the second example features a degeneration of the nonregular case with the coincidence set consisting of a single point. We note that both examples involve a given shift control u^d, i.e., the objective functional is of the form

$$J(y,u) = \frac{1}{2}\|y-z\|^2_{0,\Omega} + \frac{\alpha}{2}\|u-u^d\|^2_{0,\Omega}.$$

This generalization is easily accommodated by the theory, since the shift control can be formally absorbed by the right-hand side of the state equation.

Example 1: The data of the problem are as follows

$$\Omega := (-2,2)^2, \quad z := y^*(r) \,+\, \Delta p^*(r) \,+\, \lambda^*(r), \quad u^d := u^*(r) + \alpha^{-1}\, p^*(r)\,,$$
$$b := 0, \quad \alpha := 0.1, \quad c = 0, \quad \Gamma_D := \partial\Omega\,.$$

Here, $y^* = y^*(r), u^* = u^*(r), p^* = p^*(r)$, and $\lambda^* = \lambda^*(r), r := (x_1^2 + x_2^2)^{1/2}, (x_1,x_2)^T \in \Omega$, are chosen according to

$$y^*(r) := -r^{\frac{4}{3}}\,\gamma_1(r) \quad , \quad u^*(r) := -\Delta\, y^*(r)\,,$$
$$p^*(r) := \gamma_2(r)\,(r^4 - \frac{3}{2}r^3 + \frac{9}{16}r^2) \quad , \quad \lambda^*(r) := \begin{cases} 0\,, r < 0.75, \\ 0.1\,, \text{otherwise}, \end{cases}$$

where

$$\gamma_1 := \begin{cases} 1, & r < 0.25, \\ -192(r-0.25)^5 + 240(r-0.25)^4 - 80(r-0.25)^3 + 1, & 0.25 < r < 0.75, \\ 0, & \text{otherwise}, \end{cases},$$

$$\gamma_2 := \begin{cases} 1, & r < 0.75, \\ 0, & \text{otherwise}. \end{cases}$$

We note that the constraint b does not satisfy (1.1). However, it is easy to check that the above functions satisfy the optimality conditions (1.2a)-(1.2c).

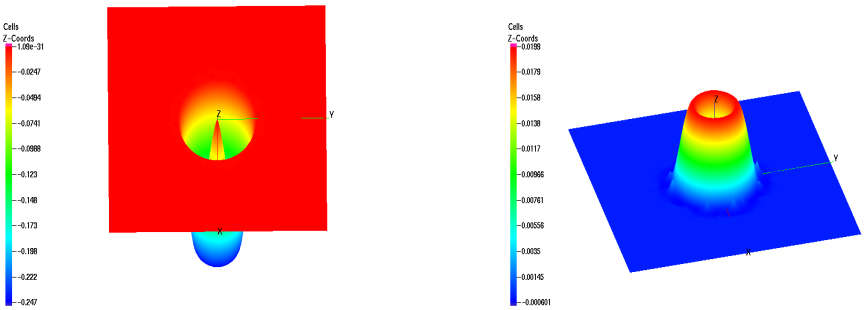

FIG. 5.1. *Example 1: Optimal state y^* (left) and optimal adjoint state p^* (right)*

The optimal state y^* is strongly oscillating around the origin with the coincidence set given by $\mathcal{A}^* = \{(r,\varphi) | 0.25 < r < 1\}$. Both y^* and p^* are displayed in Figure 5.1.

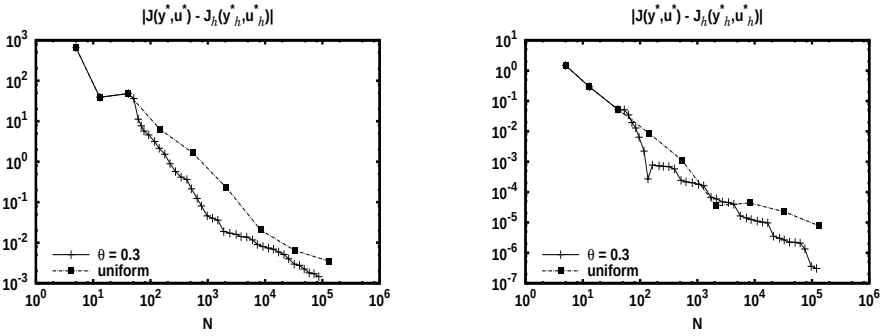

FIG. 5.2. *Decrease of the error in the objective functional as a function of the degrees of freedom for adaptive refinement ($\theta = 0.3$) and uniform refinement: Example 1 (left) and Example 2 (right))*

The performance of the adaptive algorithm is illustrated in Figure 5.2 (left) where the error in the quantity of interest (objective functional) $|J(y^*, u^*) - J_h(y_h^*, u_h^*)|$ is displayed on a logarithmic scale as a function of the total number of degrees of freedom both for adaptive refinement ($\theta = 0.3$) and uniform refinement. Although there is a benefit of adaptive refinement, the slopes of the curves are almost the same which is due to the smoothness of the optimal solution in this example.

Example 2: The data of the problem are as follows

$$\Omega := B(0,1), \quad \Gamma_D = \emptyset, \quad y^d(r) := 4 + \frac{1}{\pi} - \frac{1}{4\pi} r^2 + \frac{1}{2\pi} \ln(r)\,,$$
$$u^d(r) := 4 + \frac{1}{4\pi} r^2 - \frac{1}{2\pi} \ln(r), \quad \alpha := 1.0, \quad b(r) := r + 4\,.$$

The optimal solution is given by:

$$y^*(r) = 4, \quad p^*(r) = \frac{1}{4\pi} r^2 - \frac{1}{2\pi} \ln(r), \quad u^*(r) = 4, \quad \lambda^* = \delta_0.$$

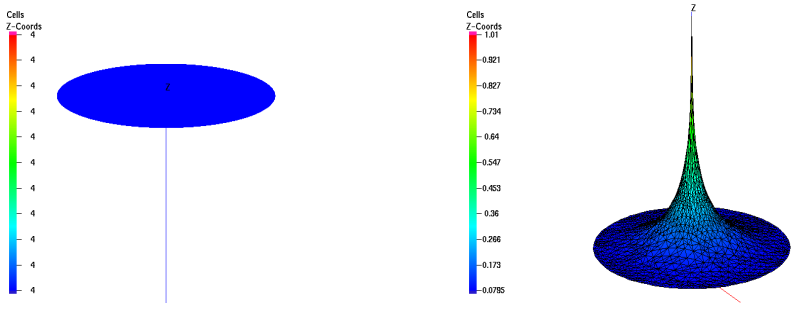

FIG. 5.3. *Example 2: The computed optimal state y_h^* (left) and the optimal adjoint state p_h^* (right)*

Visualizations of the computed optimal state y_h^* and the optimal adjoint state p_h^* are provided in Figure 5.3. The adjoint state p^* has a singularity at the origin. We note that the peak of y_h^* at the origin which can be observed in Figure 5.3 (left) is a numerical artefact due to that singularity.

Figure 5.2 (right) shows the error in the objective functional for adaptive ($\theta = 0.3$) and uniform refinement as a function of the total number of degrees of freedom. The expected optimal slopes of the curves are reached in the asymptotic regime.

REFERENCES

[1] W. BANGERTH, AND R. RANNACHER. *Adaptive Finite Element Methods for Differential Equations*. Birkhäuser Publisher, Zürich, 2003.

[2] R. BECKER AND R. RANNACHER. An optimal control approach to error estimation and mesh adaptation in finite element methods. Acta Numerica, 1–101, 2001.

[3] M. BERGOUNIOUX, M. HADDOU, M. HINTERMÜLLER, AND K. KUNISCH. A comparison of a Moreau-Yosida based active set strategy and interior point methods for constrained optimal control problems. SIAM J. Optim. **11**, 495–521, 2000.

[4] M. BERGOUNIOUX AND K. KUNISCH. On the structure of Lagrange multipliers for state constrained optimal control problems. Systems Control Lett., **48**, 169–176, 2003.

[5] R. BECKER, H. KAPP, AND R. RANNACHER. Adaptive finite element methods for optimal control of partial differential equations: basic concept. SIAM J. Control Optim., **39**, 113–132, 2000.

[6] E. CASAS. Boundary control of semilinear elliptic equations with pointwise state constraints. SIAM J. Control and Optimization, **31**, 993–1006, 1993.

[7] K. DECKELNICK AND M. HINZE. Convergence of a finite element approximation to a state constrained elliptic control problem. SIAM J. Numer. Anal., **45**, 1937–1953, 2007.

[8] W. DÖRFLER. A convergent adaptive algorithm for Poisson's equation. SIAM J. Numer. Anal., **33**, 1106–1124, 1996.

[9] K. ERIKSON, D. ESTEP, P. HANSBO, AND C. JOHNSON. Introduction to adaptive methods for differential equations. Acta Numerica, 105–158, 1995.

[10] A. GÜNTHER AND M. HINZE. A posteriori error control of a state constrained elliptic control problem. J. Numer. Math., **16**, 307–322, 2008.

[11] M. HINTERMÜLLER AND R.H.W. HOPPE. Goal-oriented adaptivity in control constrained optimal control of partial differential equations. SIAM J. Control Optim., **47**, 1721–1743, 2008.

[12] M. HINTERMÜLLER AND R.H.W. HOPPE. Goal oriented mesh adaptivity for mixed control-state constrained elliptic optimal control problems. In: Proc. Int. Conf. on Sci. Comput in Simulation, Optimization and Control, Jyväskyl, Finland, June 14-16, 2007 (W. Fitzgibbon et al.; eds) (in press)

[13] M. HINTERMÜLLER, R.H.W. HOPPE, Y. ILIASH, AND M. KIEWEG. An a posteriori error analysis of adaptive finite element methods for distributed elliptic control problems with control constraints. ESAIM: Control, Optimisation and Calculus of Variations, **14**, 540–560, 2008.

[14] M. HINTERMÜLLER AND K. KUNISCH. Feasible and non-interior path-following in constrained minimization with low multiplier regularity. SIAM J. Control and Optimization, **45**, 1198–1221, 2006.

[15] M. HINTERMÜLLER AND K. KUNISCH. Stationary optimal control problems with pointwise state constraints. to appear in: Numerical PDE Constrained Optimization (M. Heinkenschloss et al.; eds.), Lect. Notes Comput. Sci. Engrg., **Vol. 72**, Springer, Berlin-Heidelberg-New York, 2009.

[16] R.H.W. HOPPE AND M. KIEWEG. Adaptive finite element methods for mixed control-state constrained optimal control problems for elliptic boundary value problems. Computational Optimization and Applications, DOI10.1007/s10589-008-9195-4, 2008.

[17] R. LI, W. LIU, H. MA, AND T. TANG. Adaptive finite element approximation for distributed elliptic optimal control problems. SIAM J. Control Optim., **41**, 1321–1349, 2002.

[18] C. MEYER, U. PRÜFERT, AND F. TRÖLTZSCH. On two numerical methods for state-constrained elliptic problems. Optimization Methods and Software **22**, 871–899, 2007.

[19] L.R. SCOTT AND S. ZHANG. Finite element interpolation of non-smooth functions satisfying boundary conditions. Math. Comp., **54**, 483–493, 1990.

[20] B. VEXLER AND W. WOLLNER. Adaptive finite elements for elliptic optimization problems with control constraints. SIAM J. Control Optim., **47**, 1150–1177, 2008.